Solute-Atom Segregation: An Oscillatory Ni Profile at an Internal Interface in Pt(Ni)

S.-M. Kuo, A. Seki,[a] Y. Oh, and D. N. Seidman[b]
Materials Science and Engineering Department, Northwestern University, Evanston, Illinois 60208-3108
(Received 9 April 1990)

Thermodynamic equilibrium segregation at an individual grain boundary in a Pt-3 at.% Ni alloy is studied via transmission electron microscopy, atom-probe field-ion microscopy, and Monte Carlo simulations. Ni segregation is measured at the grain boundary. The Ni concentration profile is asymmetric with respect to the grain-boundary plane; it decreases in an oscillatory fashion on one side and monotonically on the other side.

PACS numbers: 61.70.Ng, 02.50.+s, 61.16.Fk, 64.75.+g

Grain boundaries (GB's) can be treated using classical thermodynamics,[1-3] where the thermodynamic state of a GB depends on the standard variables plus the geometric variables required to describe the interface between two grains.[2,3] The state of knowledge of phase equilibria and phase transitions at internal interfaces[2-6] lags far behind our knowledge of analogous phenomena at solid-vacuum (or gas) interfaces.[7] As part of our effort to study solute-atom segregation and phase transitions on an atomic scale at individual GB's, a combined approach employing transmission electron microscopy (TEM), atom-probe field-ion microscopy (APFIM), and Monte Carlo (MC) computer simulations is utilized. In parallel with the experimental work we perform MC simulations employing embedded atom method (EAM) potentials.[8-10] The work presented here represents the first time that all three techniques have been applied to the *same* GB; the system studied is a Pt-3 at.% Ni alloy in a primary solid-solution phase field.

Pt-3 at.% Ni wires (0.15 mm diam) were sealed in a quartz capsule at 800 Pa Ar, after the capsule had been flushed with argon. The specimens were annealed at 850 K for 24 h to induce Ni segregation at GB's, and then quenched into a saturated-brine solution at 273 K. This results in a root-mean-square diffusion distance of >20 nm for Ni atoms; hence, at the very least, there is local thermodynamic equilibrium of Ni atoms with GB's. A wire was electroetched to a pointed tip (≈ 10 nm radius) that was suitable for both TEM and APFIM.[11] After electroetching it was mounted in a special double-tilt stage for a 200-kV TEM, and a GB was located and analyzed crystallographically. Next, it was backpolished to place the GB in the tip of the specimen.[11-14]

The 5 macroscopic degrees of freedom of a GB are specified by the unit vector (**c**) about which one grain is rotated with respect to a second, the rotation angle (θ) about **c**, and the outward unit normal (**n**) to the plane of the GB.[15-17] This information is obtained from Kikuchi patterns of adjacent grains at the same tilt angle; the procedure is repeated for different tilt angles. The Kikuchi patterns are matched with computer simulated patterns to determine the directions of the electron beam and subsequently θ. Four patterns, two for each grain, are required to determine **c** and θ; three sets of patterns, however, are used to check for self-consistency. The beam direction and tilt axis are used as invariant directions to calculate **c** and θ; the spread in **c** or θ is $<0.5°$. The vector **n** is determined by rotating and tilting until a minimum in the projected width of a GB is achieved; bright-field images and Kikuchi patterns are employed to calculate **n**. The quantities $\mathbf{n}_1$ and $\mathbf{n}_2$ are the outward unit normals to a GB plane in grains 1 and 2 (G1 and G2); they are related to one another via the rotation matrix $\mathbf{R}'$, i.e., by the equation $\mathbf{n}_2=\mathbf{R}'\mathbf{n}_1$. Once $\mathbf{n}_1$ and $\mathbf{R}'$ are measured $\mathbf{n}_2$ can be calculated; in practice $\mathbf{n}_2$ is also determined and compared with the calculated value. The difference between the two values of $\mathbf{n}_2$ is $<2°$. Based on the 24 symmetry operations, the $\mathbf{R}'$ associated with smallest value of θ is chosen for comparison with nearest coincidence site lattice (CSL) orientation.[16] From $\mathbf{R}'$ the following are determined: $\mathbf{c}=[0.995, 0.083, 0.057]$ and $\theta=37.27°$; **c** is 5.84° from [100]. The normal $\mathbf{n}_1$ is $[0.70, -0.076, 0.71]_1$ and it is 4.26° from [101]; thus the plane of the GB is $\approx(202)$. The angle between $\mathbf{n}_1$ (or $\mathbf{n}_2$) and **c** is $\approx 45°$; this implies it is halfway between a pure tilt and a pure twist GB. $\mathbf{R}'$ is the product of the rotation matrix for the exact CSL orientation ($\mathbf{R}$) and the matrix for the small angular deviation [$\mathbf{R}(02)$] from exact coincidence,[17] i.e., $\mathbf{R}'=\mathbf{R}(02)\mathbf{R}$. $\mathbf{R}(02)$ corresponds to a deviation of 3.72° about the [0.062,0.61,0.79] axis from the $\Sigma=5$ CSL orientation. (For a $\Sigma=5$ CSL orientation **c** is [100] and $\theta=36.87°$.) $\mathbf{R}'$ and $\mathbf{n}_1$ describe a $\Sigma\approx 5$ CSL, with a deviation angle ($\Delta\theta$) from coincidence of $\Delta\theta=0.4°$.

The same GB was next analyzed by the APFIM technique and the results are exhibited in Fig. 1. Each plot is an integral profile; i.e., the cumulative number of Ni atoms (ordinate) versus the cumulative number of Pt plus Ni atoms (abscissa). The smallest vertical or horizontal line represents a *single* atom. Figure 1(a) is a control run of the matrix concentration far from the GB. The slope of the straight line drawn from the origin through the last data point is equal to the average matrix Ni concentration, $\langle C_{\mathrm{Ni}}\rangle$. The local fluctuations about $\langle C_{\mathrm{Ni}}\rangle$ represent random solid-state fluctuations, due to the size of the sample; for these data $\langle C_{\mathrm{Ni}}\rangle$ is 2.9 ± 0.2

© 1990 The American Physical Society

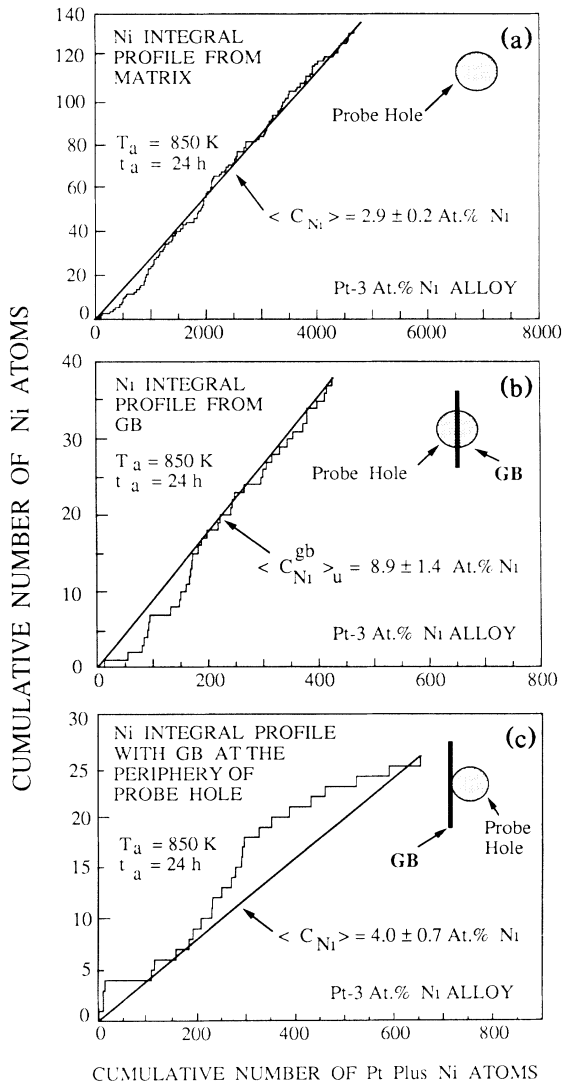

FIG. 1. (a)–(c) Three Ni integral profiles obtained employing a pulse fraction voltage of 15%, a specimen temperature of 45 K, and a vacuum of 6.7×10^{-8} Pa in the APFIM; the probe hole diameter is 1.4 nm.

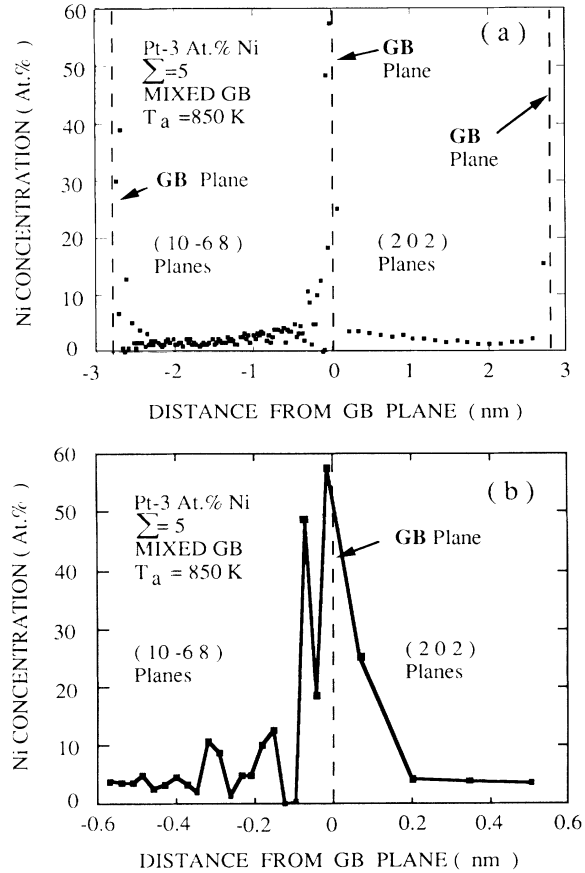

FIG. 2. (a) The Ni concentration (at.%) vs distance (nm) from the GB plane for the bicrystal. The profile repeats itself because of periodic boundary conditions. (b) A blowup of the immediate vicinity of the GB plane.

at.%. Figure 1(b) was recorded with the probe hole centered symmetrically with respect to the GB plane; the mean slope is $\langle C^{gb}_{Ni}\rangle_u = 8.9\pm1.4$ at.% Ni. This value is the *uncorrected* Ni concentration of the GB, and it is ≈ 3.07 times greater than $\langle C_{Ni}\rangle$; this represents a *minimum* value for the segregation enhancement factor, because of the matrix contribution. Figure 1(c) was recorded with the GB placed at the periphery of the projection of the probe hole; the measured Ni concentration is 4.0 ± 0.8 at.% Ni for this geometry. The latter value is $\approx 33\% > \langle C_{Ni}\rangle$, and this implies that the concentration profile associated with this GB is broadened. For the geometries employed in Fig. 1 the measured diameter of the cylinder of alloy analyzed is *only* 1.4 nm, and the plane of the GB is normal to the page.

Next the MC technique was employed to simulate Ni segregation at this GB, at 850 K, for a $\Sigma=5$ CSL orientation and (202) GB plane. The computer-generated bicrystal consists of 20 (202) planes with each plane containing 100 atoms (G1), and 100 $(10\bar{6}8)$ planes with each plane containing 20 atoms (G2); this bicrystal has 4000 atoms. Three-dimensional periodic boundary conditions and EAM potentials for Pt and Ni were employed.[8-10] The EAM potentials have been used to study segregation at surfaces,[8] dislocations,[18] twist boundaries,[19] and twins[20] in dilute fcc alloys.

During an MC simulation the total number of atoms and the chemical potential difference between the Pt and Ni atoms in the bicrystal is fixed, as well as the pressure and temperature. Four different steps[8,19] are employed in these simulations: (i) individual atoms are displaced; (ii) the total volume of the bicrystal is changed *after* each atom in the bicrystal has undergone one MC step; (iii) solvent and solute atoms are exchanged; and (iv) one grain is allowed to translate with respect to the other grain. With these steps the relaxation and thermal motion of atoms are included, as well as compositional

variations between the bulk of the bicrystal and the interfacial region between G1 and G2. To decide whether or not a trial configuration is accepted, the Metropolis *et al.* algorithm[21] is employed. After achieving an equilibrium state (≈ 375 MC steps per atom for the 4000 atoms) the number of solute atoms in each plane that is parallel to the GB, and their atomic positions, are averaged over the next ≈ 500 to 1250 MC steps per atom.

The Ni concentration profile is exhibited in Fig. 2; the profile of the entire bicrystal is exhibited in Fig. 2(a) —the profile repeats itself as a result of the periodic boundary conditions. Figure 2(b) is a blowup of the region in the immediate vicinity of the interface; N.B., there is *not* an atomic plane at the position denoted GB. This profile shows that the Ni concentration at the (202) plane immediately to the right of the GB (G1) has a concentration of 25.1 at.% Ni, and the Ni concentration falls monotonically to the matrix value in the second (202) plane, i.e., at 0.174 nm from the interface plane. The $(10\bar{6}8)$ plane immediately to the left of the GB plane (G2) has a concentration of 57.4 at.% Ni. Instead of the Ni concentration decreasing monotonically to the matrix value it oscillates for at least 15 $(10\bar{6}8)$ planes (≈ 0.416 nm) before reaching ≈ 3 at.% Ni. The oscillatory Ni concentration profile is the first observation of this type of segregation behavior at a GB. Another point is that the Ni profile is asymmetric with respect to the GB plane; this asymmetry demonstrates that the structure of a GB affects its segregation behavior.

Finally, the MC results allow us to interpret the measured concentration values (Fig. 1). Figure 3 exhibits schematic diagrams of the experimental situation in Fig. 1, with the probe hole superimposed on the lattice planes. Case I corresponds to the experimental situation of Fig. 1(b); the $(10\bar{6}8)$ planes are to the left of the GB and the (202) planes to the right side; the probe hole covers 5 (202) and 23 $(10\bar{6}8)$ planes. Case II corresponds to the experimental situation of Fig. 1(c); the probe hole covers 10 (202) planes. The MC simulation results were then used to calculate the mean Ni concentration for the two cases in Fig. 3; the length of each plane (y_i) included within the probe hole and its calculated Ni concentration were taken into account. For case I the calculated Ni concentration is 9.75 at.%, as compared to an experimental value of 8.9 ± 1.4 at.% Ni; and in case II the calculated Ni concentration is 4.1 at.%, as compared to the experimental value of 4.0 ± 0.7 at.% Ni. Thus the calculated Ni concentrations are in very good agreement with the experimental values; this lends credence to the existence of an oscillatory Ni concentration profile, as observed in the MC simulations.

This is the first observation of an oscillatory Ni segregation profile at a GB. Prior observations, however, of oscillatory profiles have been observed by low-energy electron diffraction, and also calculated for the (111) and (110) solid-vacuum surfaces of Pt-Ni alloys.[22-26] [Also, oscillatory segregation profiles have been detected

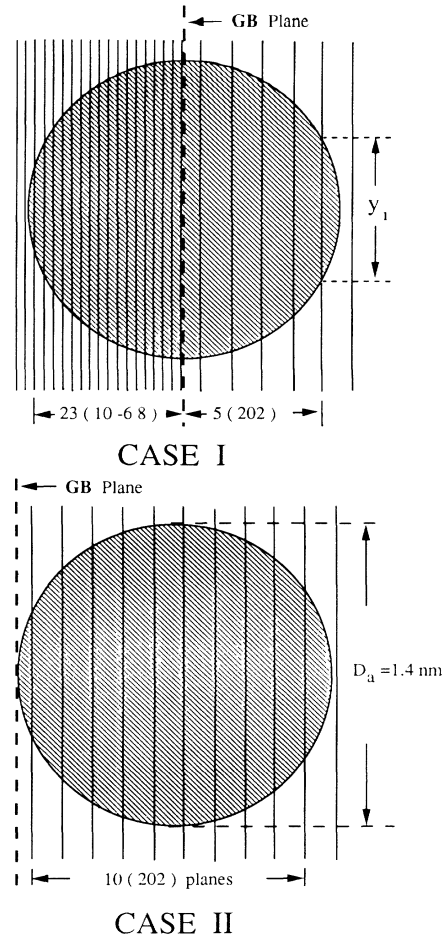

FIG. 3. These diagrams exhibit the geometry and crystallography corresponding to Figs. 1(b) and 1(c). The symbol y_i indicates the length of each plane within the 1.4-nm-diam probe hole. The vertical lines symbolize end-on views of the planes.

at the solid-vacuum surfaces of Ni-Cu, Pt-Rh, Pt-Ru, Pt-Rh-S, and Pt-Ru-S alloys by APFIM;[27-29] and recently discovered via Monte Carlo simulations at the Si-Ge(100)2×1 solid-vacuum surface.[30]] In the case of the GB studied the $(10\bar{6}8)$ planes are vicinal to $(1\bar{1}1)$ planes. The angle between these two sets of planes is $\approx 11.5°$; and within the context of the ledge-kink-terrace model the $(1\bar{1}1)$ terraces are ≈ 1.1 nm wide for a ledge height equal to 0.226 nm. Thus the oscillatory segregation behavior for the $(10\bar{6}8)$ planes straddling this GB is analogous qualitatively to the oscillatory behavior observed at the (111) solid-vacuum surface; the (111) solid-vacuum surface plane is, however, enriched in Pt, while the first $(10\bar{6}8)$ plane to the left of the GB is enriched in Ni.

In conclusion, we have combined TEM, APFIM, and MC computer simulations to study Ni segregation at an individual GB in a single-phase Pt-3 at.% alloy. TEM is used to determine the 5 macroscopic degrees of freedom

of a GB, and APFIM is employed to measure its chemical composition; it is a $\Sigma \approx 5$ CSL/$\approx$(202) GB. MC computer simulations are also used to simulate Ni segregation at the *same* GB; and the calculated values are in good agreement with the experimentally determined Ni concentrations. They also indicate that the distribution of Ni atoms is asymmetric with respect to the GB plane; on the (202) side the Ni profile decreases monotonically and on the $(10\bar{6}8)$ side it decreases in an oscillatory fashion. This asymmetric Ni concentration profile demonstrates that the atomic structure of a GB affects the segregation behavior.

This research is supported by NSF Grant No. DMR-8819074. It utilized central facilities of the NSF funded Materials Research Center at Northwestern University. The Monte Carlo simulations were performed at the NSF funded Pittsburgh Supercomputing Center. A.S. was supported by Sumitomo Metal Industries, Ltd. We thank the following for useful discussions: S. M. Foiles; K. L. Merkle; P. Haasen and L. Alvensleben (Göttingen) [made possible by a von Humboldt Senior Fellowship (D.N.S.)]; and G. Martin, B. Legrand, and V. Pontikis (Saclay) [made possible by an International NSF grant to D.N.S.].

[a]Current address: Sumitomo Metal Industries, Ltd., Research and Development Division, Osaka, Japan.

[b]To whom correspondence should be addressed.

[1]E. W. Hart, in *The Nature and Behavior of Grain Boundaries,* edited by Hsun Hu (Plenum, New York, 1972), p. 155.

[2]J. W. Cahn, J. Phys. (Paris), Colloq. **43**, C6-199 (1982).

[3]C. Rottman, J. Phys. (Paris), Colloq. **49**, C5-313 (1988).

[4]V. Pontikis, J. Phys. (Paris), Colloq. **49**, C5-327 (1988).

[5]T. E. Hsieh and R. W. Balluffi, Acta Metall. **37**, 1637 (1989).

[6]E. L. Maksimova, E. I. Rabinkin, L. S. Shvindlerman, and B. B. Straumal, Acta Metall. **37**, 1995 (1989).

[7]J. M. Blakely, J. Phys. (Paris), Colloq. **49**, C5-351 (1988).

[8]S. M. Foiles, Phys. Rev. B **32**, 7685 (1985).

[9]S. M. Foiles, M. I. Baskes, and M. S. Daw, Phys. Rev. B **33**, 7983 (1986).

[10]M. S. Daw, Phys. Rev. B **39**, 7441 (1989).

[11]J. G. Hu, B. W. Krakauer, S.-M. Kuo, R. Mallick, A. Seki, D. N. Seidman, J. Baker, and R. Loyd (to be published).

[12]B. Loberg and H. Nordén, Arkiv. Fys. **39**, 383 (1969).

[13]D. N. Seidman, Mater. Res. Soc. Symp. Proc. **138**, 315 (1989); J. G. Hu, S.-M. Kuo, A. Seki, B. W. Krakauer, and D. N. Seidman, Scr. Metall. **23**, 2013 (1989).

[14]L. V. Alvensleben and P. Haasen, Mater. Res. Soc. Symp. Proc. **138**, 479 (1989).

[15]W. T. Read, Jr., and W. Shockley, Phys. Rev. **78**, 275 (1950).

[16]W. Bollmann, *Crystal Lattices, Interfaces, Matrices* (Imprimerie des Bergues, Geneva, 1982), p. 336.

[17]W. Bollmann, B. Michaut, and G. Sainfort, Phys. Status Solidi (a) **13**, 637 (1972).

[18]S. M. Foiles, Mater. Res. Soc. Symp. Proc. **63**, 61 (1985); Phys. Rev. B **40**, 11 502 (1989).

[19]A. Seki, D. N. Seidman, Y. Oh, and S. M. Foiles (to be published).

[20]M. Ueno, A. Seki, Y. Oh, and D. N. Seidman (to be published).

[21]N. Metropolis, M. N. Rosenbluth, A. W. Rosenbluth, A. H. Teller, and E. Teller, J. Chem. Phys. **21**, 1087 (1953).

[22]Y. Gauthier, Y. Joly, R. Baudoing, and J. Rundgren, Phys. Rev. B **31**, 6216 (1985).

[23]R. Baudoing, Y. Gauthier, M. Lundberg, and J. Rundgren, J. Phys. C **19**, 2825 (1986).

[24]G. Tréglia and B. Legrand, Phys. Rev. B **35**, 4338 (1987).

[25]Y. Gauthier, R. Baudoing, M. Lundberg, and J. Rundgren, Phys. Rev. B **35**, 7876 (1987).

[26]M. Lundberg, Phys. Rev. B **36**, 4692 (1987).

[27]Y. S. Ng, T. T. Tsong, and S. B. McLane, Phys. Rev. Lett. **42**, 588 (1979).

[28]M. Ahmad and T. T. Tsong, J. Chem. Phys. **83**, 388 (1985).

[29]T. T. Tsong, D. M. Ren, and M. Ahmad, Phys. Rev. B **38**, 7428 (1988).

[30]P. C. Kelires and J. Tersoff, Phys. Rev. Lett. **63**, 1164 (1989).

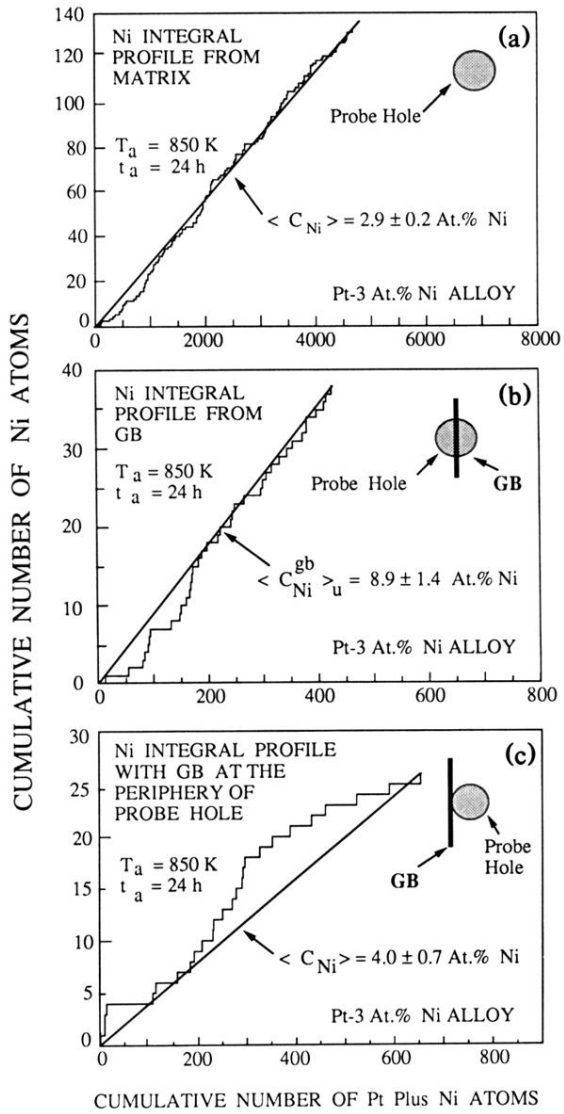

FIG. 1. (a)–(c) Three Ni integral profiles obtained employing a pulse fraction voltage of 15%, a specimen temperature of 45 K, and a vacuum of 6.7×10^{-8} Pa in the APFIM; the probe hole diameter is 1.4 nm.